International Journal of Computational Methods and Experimental Measurements
https://www.acadlore.com/journals/IJCMEM

Terrestrial Laser Scanning–Based 3D Modeling of a Corridor-Type Building Interior

Kuandyk Akshulakov[1], Askar Mustabekov[1], Aleksey Sidorov[2], Alibek Dosbossyn[3*]

[1] Research Institute of Military Art, National Defense University of the Republic of Kazakhstan, 010000 Astana, Kazakhstan
[2] Department of Geodesy and Cartography, National Defense University, 010000 Astana, Kazakhstan
[3] Warwick Business School, University of Warwick, CV4 7AL Coventry, United Kingdom

[*] Correspondence: Alibek Dosbossyn (adosbosyn04@gmail.com)

Received: 04-07-2026 **Revised:** 04-20-2026 **Accepted:** 05-19-2026

Citation: K. Akshulakov, A. Mustabekov, A. Sidorov, and A. Dosbossyn, "Terrestrial laser scanning–based 3D modeling of a corridor-type building interior," *Int. J. Comput. Methods Exp. Meas.*, vol. 14, no. 2, pp. 229–237, 2026. https://doi.org/10.56578/ijcmem140205.

Abstract: This paper presents a reproducible workflow for three-dimensional modeling of a corridor-type building interior using terrestrial laser scanning (TLS) data. It also provides a quantitative evaluation of the workflow on a real object. In contrast to studies that focus mainly on automatic segmentation or scan-to-building information modeling (BIM), this study emphasizes the reproducible integration of a field protocol, registration graph control, and two-stage quality assurance (QA). The QA procedure combines internal registration statistics with independent metric verification. The field campaign included 82 Leica BLK360 scanner setups completed within one working day. Adjacent stations were acquired with controlled overlap, and the scanning network was locally reinforced in repetitive corridor geometry. The setup height ranged from 1.40 to 1.55 m. The average working scanning distance was 5.8 m, and the maximum distance was 12.1 m. Post-processing was performed in the Leica Cyclone software ecosystem. The procedure included visual inertial system (VIS)-assisted preliminary alignment, registration graph inspection, removal of seven weak links, global optimization, combined point cloud cleaning, and final metric verification. The resulting point cloud contained more than 100 million colorized points. The final registration root mean square error (RMSE) did not exceed 5 mm. The 95th percentile of residual errors (P95) was 18 mm, and the maximum residual was 28 mm. Independent verification showed that 18 control linear dimensions measured in the point cloud agreed with in situ tape measurements within 4–5 mm. The tape measurements were performed with a nominal accuracy of ±1 mm. The main geometric parameters of the interior were confirmed: a corridor length of 77.6 m, ceiling heights of 2.96–3.02 m, angles of 92.2–92.7°, and diameters of six engineering pipes ranging from 0.04 to 0.075 m. The resulting point cloud can be used as input data for scan-to-BIM workflows and for developing digital representations of interiors, provided that the described acquisition and quality-control protocol is followed.

Keywords: Terrestrial laser scanning; Point cloud; Point cloud registration; Quality control; Metric verification; Corridor-type interiors; Scan-to-building information modeling

1 Introduction

Three-dimensional models of building interiors are increasingly used as measurable digital representations. They support inventory, reconstruction, change monitoring, preparation of design documentation, and immersive VR-based training environments. For these applications, the main requirement is not only visual quality. The model must also be geometrically consistent and supported by quantitative quality metrics.

Corridor-type interiors present a specific practical problem that is still insufficiently addressed in applied publications. Repetitive geometry, similar door openings, and long homogeneous segments increase the risk of cumulative registration drift. At the same time, many studies provide detailed discussions of automatic segmentation, building information modeling (BIM)-oriented recognition, or registration algorithms, but give less attention to reproducible field protocols and independent metric verification on real objects. Consequently, practitioners often receive a general workflow rather than operational rules and quality-control criteria that can be repeated in similar surveys.

Traditional measurements and 2D floor plans remain useful for local tasks. However, they do not provide a dense geometric description of complex spaces, and they are difficult to scale when rapid data updates are required. Photogrammetry may also be useful, but its robustness in interiors can decrease because of weak texture, uneven illumination, and reflective surfaces. Therefore, terrestrial laser scanning (TLS) remains a basic tool for constructing metrically reliable interior models.

Recent studies confirm the potential of point cloud-based workflows for as-built modeling and scan-to-BIM. They also show that these workflows depend on source point cloud quality, registration robustness, and transparent quality-control procedures [1–7]. The present paper therefore does not propose a new registration algorithm. Instead, it addresses the reproducible organization of TLS acquisition, post-processing, and verification for a corridor-type building interior.

The aim of the study was to develop and experimentally validate a reproducible workflow for 3D modeling of a corridor-type building interior from TLS data. The workflow was evaluated through documented assessment of registration accuracy and independent metric verification.

The scientific contribution of the paper is as follows:

(1) A reproducible combination of field protocol, scanning network reinforcement rules, and quality assurance/quality control (QA/QC) for repetitive corridor geometry is proposed;

(2) The practical value of independent metric verification in addition to internal registration metrics is demonstrated;

(3) Conditions for transferring the workflow to other layout schemes are formulated.

2 Literature Review

Research on indoor mapping and scan-to-BIM shows that the key limitation is not simply the availability of a point cloud. The point cloud must also be suitable for interpretation, segmentation, and as-built model generation. Macher et al. [1] showed that semi-automatic reconstruction of interiors from point clouds depends on the stability of the preliminary geometric structure and on input data quality. Rocha and Mateus [2] similarly noted that reliable BIM generation is determined by point cloud completeness and quality, whereas registration, interpretation, and parameterization remain labor-intensive stages. Gourguechon et al. [3] provided a broader overview of automated as-built BIM creation for indoor scenes and identified the integration of segmentation, recognition, and robust geometric modeling as a major bottleneck.

Recent work has also focused on the automation of registration and on linking BIM models with point clouds. Zhang et al. [4] proposed an automatic approach to global BIM–point cloud registration and association for construction progress monitoring. Their study highlighted the labor intensity of manual correspondence selection and the sensitivity of results to initial alignment quality. Liu et al. [5] examined depth-informed point cloud-to-BIM registration for construction inspection and emphasized that alignment accuracy and robustness remain critical constraints in field applications. Chen et al. [6] showed that point cloud-to-BIM registration can refine observer localization in indoor environments when reliable alignment between a partial point cloud and a BIM reference is achieved. Park et al. [7] further demonstrated that robust station alignment remains decisive even in automated stop-and-go scanning scenarios.

Automatic segmentation, parametric modeling, and topology extraction are actively developing for indoor scenes. Túñez-Alcalde et al. [8] showed that room extraction and connectivity detection remain sensitive to occlusions, data heterogeneity, and layout-specific features, even when effective algorithms are available. Hu et al. [9] demonstrated BIM-to-scan semantic segmentation using domain adaptation, which can reduce the labor required for annotating real point clouds. For interiors with engineering systems, additional progress has been made in parametric modeling of mechanical, electrical, and plumbing (MEP) elements and mobile acquisition of indoor point clouds [10, 11].

Another group of studies addresses geometric accuracy, uncertainty, and robustness in TLS models. Wang et al. [12] proposed procedures for comparing laser scanning data with reference geometry and emphasized that root mean square error (RMSE) alone is insufficient without analysis of control deviations on actual object elements. Jarząbek-Rychard and Maas [13] extended this argument for scan-to-BIM and treated geometric uncertainty as an independent component of analysis rather than a secondary effect of registration. Isfort et al. [14] demonstrated that robust multimodal point cloud registration requires explicit quantitative evaluation using datasets with different structures and densities. Applied case studies also confirm the importance of transparent TLS workflows for engineering documentation and construction asset management [15]. Cross-platform point cloud exchange is supported by the E57 standard [16], while BIM-oriented information management is framed by the principles of ISO 19650 [17].

Overall, the literature provides extensive coverage of automatic registration, segmentation, uncertainty-aware evaluation, and scan-to-BIM. However, an applied gap remains for reproducible TLS workflows in corridor-type building interiors. In such interiors, long repetitive scenes increase the risk of cumulative error. This paper addresses that gap by describing an operational field protocol, formalizing quality-control procedures, and combining internal registration statistics with independent metric measurements.

3 Materials and Methods

3.1 Study Object and Experimental Design

The study object was a one-story corridor-type building that included a corridor, vestibule, living rooms, sanitary facilities, instructional rooms, and storage rooms. The survey was completed within one working day. In total, 82 stations were acquired: 3 in the vestibule, 20 in the corridor, 30 in living rooms, 12 in sanitary facilities, and 17 in instructional and storage areas. This configuration provided coverage of both extended homogeneous segments and local rooms with complex geometry and dense engineering elements.

3.2 Equipment and Software Environment

A Leica BLK360 scanner was used during the field stage. According to the manufacturer's technical documentation, the device includes a visual inertial system (VIS) that supports automatic preliminary alignment of adjacent stations under field conditions. Its specified ranging accuracy is 4 mm at distances up to 10 m [18]. Post-processing was performed in the Leica Cyclone FIELD 360, REGISTER 360 PLUS, Cyclone 3DR, and TruView software environment. Because this study did not evaluate Leica's proprietary algorithms, the software ecosystem was treated as an applied tool. The analysis focused on reproducible user-level decisions, including scanning route configuration, network reinforcement, registration graph inspection, cleaning, and independent verification.

3.3 Field Protocol and Scanning Network Planning

Each station was labeled from S001 to S082. For each setup, the station position, route logic, tripod height, illumination conditions, reflective surfaces, and the need for an additional station were recorded. The basic planning rule was to maintain at least 30–40% overlap between adjacent stations. In repetitive corridor zones and in rooms with complex engineering systems, the network was locally reinforced to approximately 50% overlap.

The setup height ranged from 1.40 to 1.55 m. This range reduced shadow zones in the lower part of the interior and preserved visibility of door openings, corners, columns, and engineering elements used as natural geometric anchors. The average time per setup was 45–50 s, which allowed the acquisition cycle to be completed within one working day.

In this workflow, VIS was used for preliminary linking of consecutive stations along the scanner trajectory. The registration graph was then checked in the office, followed by global project optimization. The field stage and post-acquisition registration were therefore treated as connected parts of a single workflow.

3.4 Post-Processing, Registration, and Point Cloud Cleaning

The post-processing pipeline included project import, structuring by zones, VIS-assisted preliminary alignment, registration graph inspection, exclusion of weak or doubtful links, global optimization, point cloud cleaning, final metric verification, and export to E57, RCP/RCS, and OBJ/FBX formats. After inspection of the registration graph, seven weak links that reduced the stability of the global alignment were removed.

Processing reproducibility was supported by recording the key user decisions made during registration and cleaning. These decisions included graph inspection, removal of weak station links, and the use of combined point cloud cleaning.

Point cloud cleaning was performed in a combined manual and semi-automatic mode. First, zonal cropping and removal of irrelevant areas were carried out. Temporary objects and dynamic elements were then removed. Finally, residual noise, reflections, and local artifacts in problematic areas were checked manually.

This combined approach reduced routine processing while preserving user control in areas where automatic procedures may be sensitive to reflective surfaces and repetitive geometry.

3.5 Mathematical Formulation and Accuracy Metrics

The coordinate transformation of points during pairwise scan registration was defined by a rigid transformation:

$$p_i' = Rp_i + t \tag{1}$$

where, p_i is the original point of the i-th scan, p_i' is the transformed point, R is the rotation matrix, and t is the translation vector.

The general registration problem was formulated as minimization of the squared residual distances between corresponding geometric elements:

$$\min_{R,t} \Sigma_k \left\| Rp_k + t - q_k \right\|^2 \tag{2}$$

where, q_k is the corresponding point or geometric element in the paired scan, and k denotes the set of admissible correspondences.

The integral registration quality metric was defined by the RMSE:

$$\text{RMSE} = \sqrt{\frac{1}{n}\Sigma_k d_k^2} \tag{3}$$

where, d_k is the residual deviation for the k-th correspondence, and n is the number of correspondences included in the evaluation.

For independent verification of linear dimensions, the absolute difference between the point cloud measurement and the in situ tape measurement was calculated as follows:

$$\Delta L_i = \left| L_i^{\text{cloud}} - L_i^{\text{field}} \right| \tag{4}$$

The relative error was defined as:

$$\delta L_i = \frac{\Delta L_i}{L_i^{\text{field}}} \times 100\% \tag{5}$$

For angular characteristics, the angle between the normals of two planes was estimated as:

$$\theta = \arccos\left(\frac{n_1 \cdot n_2}{\|n_1\| \, \|n_2\|}\right) \tag{6}$$

In addition to RMSE, the maximum residual and the 95th percentile of residual errors were used to characterize registration stability. These indicators help identify local outliers that may be critical for engineering interpretation of the model.

According to the registration report, the 95th percentile of residual errors was 18 mm, and the maximum registration residual was 28 mm.

3.6 Protocol for Independent Metric Verification

Independent metric verification was performed using 18 control geometric elements distributed across different zones of the object. These elements included longitudinal corridor segments, height dimensions, local engineering elements, and selected transverse cross-sections.

In situ measurements were made using a tape measure with a nominal accuracy of ±1 mm. The control set was used to assess metric consistency both within individual rooms and along the extended corridor structure.

The verification protocol provides a reproducible basis for interpreting differences between the point cloud and the in situ measurements.

As shown in Figure 1, all recorded control measurement errors were within the 4–5 mm range. This distribution confirms the practical metric reliability of the TLS-based model. The mean error was 4.39 mm.

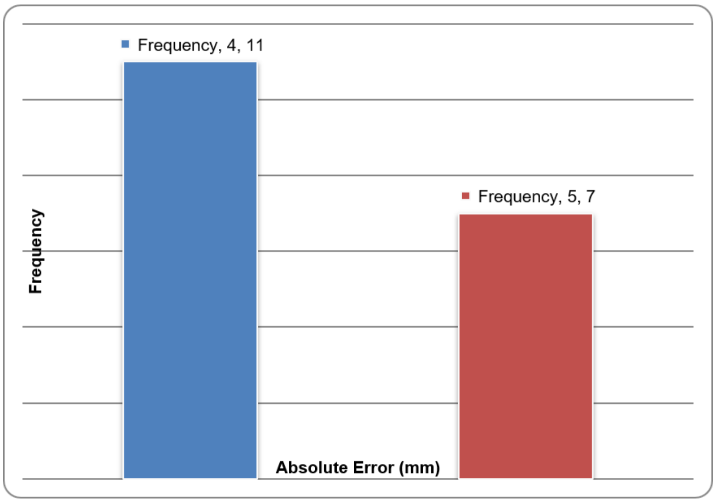

Figure 1. Histogram of absolute control measurement errors

4 Results

4.1 Completeness and Structure of the Point Cloud

The survey produced a complete point cloud of the interior spaces containing more than 100 million colorized points. The spatial coverage was sufficient to reconstruct the continuous geometry of the corridor, rooms, sanitary facilities, and engineering utility areas. The main acquisition parameters are summarized in Table 1.

Table 1. Field protocol and scope of work

Parameter	Value
Number of setups	82
Overlap between adjacent setups	30–40% (up to 50% in complex zones)
Setup height	1.40–1.55 m
Average time per setup	45–50 s
Point cloud volume	>100 million points
Average working distance	5.8 m
Maximum working distance	12.1 m

4.2 Registration Accuracy

The final registration RMSE did not exceed 5 mm. For a corridor-type interior, this result indicates metric consistency and shows that the selected traversal scheme and network reinforcement strategy prevented noticeable cumulative drift along extended homogeneous segments.

The average working scanning distance was approximately 5.8 m, and the maximum distance was 12.1 m.

These working distances are consistent with the BLK360 specification. They also explain why the final RMSE was comparable to the instrument accuracy at short and medium ranges. The complete set of accuracy metrics is presented in Table 2.

Table 2. Accuracy metrics

Metric	Value
Registration root mean square error (RMSE)	$\leq$5 mm
Control measurements (point cloud vs. field)	4–5 mm
95th percentile of residual errors	18 mm
Maximum residual	28 mm
Number of control measurements	18
Tape measure accuracy	$\pm$1 mm

4.3 Independent Metric Verification

Linear dimensions measured in the point cloud in TruView/Cyclone 3DR were compared with 18 in situ measurements made using a tape measure with a nominal accuracy of ±1 mm. The discrepancies were within 4–5 mm. This result is consistent with the internal registration statistics and confirms the suitability of the point cloud for engineering measurements.

The control measurements were distributed across the main zones of the object and included representative linear elements for assessing the metric reliability of the final point cloud.

Additional registration stability indicators were P95 = 18 mm and a maximum residual of 28 mm. These values indicate isolated local outliers, but they do not change the overall conclusion regarding the metric suitability of the final point cloud for engineering interpretation.

4.4 Verified Geometric Parameters

The final model confirmed the following geometric parameters: total corridor length of 77.6 m, ceiling height of 2.96–3.02 m, angles between conjugate planes of 92.2–92.7°, and engineering pipe diameters of 0.04–0.075 m.

Engineering pipe diameters were determined from six measured pipes distributed across different zones of the object. The verified geometric parameters are presented in Table 3.

Table 3. Control geometric parameters

Parameter	Value	Note
Corridor length	77.6 m	Confirmed by control measurements
Ceiling height	2.96–3.02 m	Range across different sections
Angles between planes	92.2–92.7°	Estimated from plane normals
Pipe diameters	0.04–0.075 m	Number of measured pipes: 6

4.5 Export and Cross-Platform Portability

The final dataset was prepared for transfer in E57, RCP/RCS, and OBJ/FBX formats. In this study, these formats ensured cross-platform portability of the point cloud. The correct interpretation of the result is that the point cloud is suitable as input data for scan-to-BIM procedures and for the subsequent digital representation of the interior. The point cloud itself is not equivalent to a BIM model and does not constitute a complete digital twin.

4.6 Illustrative Material

The illustrative material follows the sequence of the workflow. Figure 2 shows the scan station layout and overlap zones. Figure 3 presents the registration connectivity graph. Figure 4 provides examples of control measurements in TruView/Cyclone 3DR. Figure 5 shows the final 3D model of the corridor interior with a control measurement example. Together, these figures support a comparison of the field acquisition configuration, registration quality, and metric verification results.

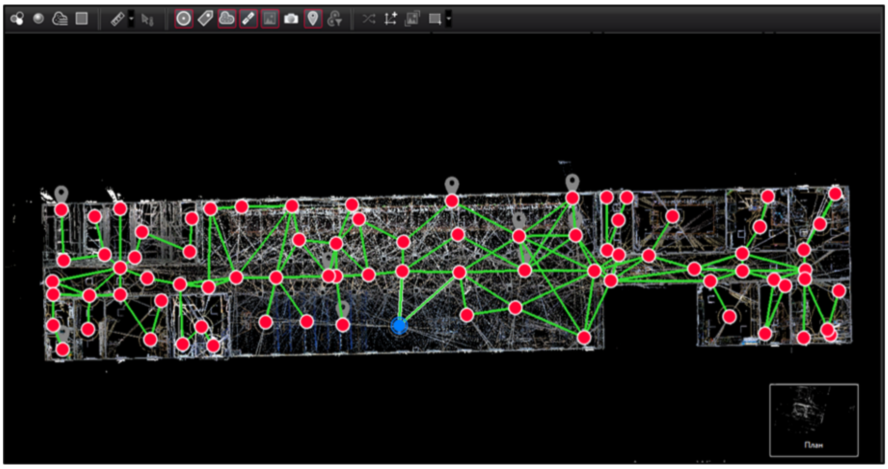

Figure 2. Layout of scan stations (S001–S082) and overlap zones

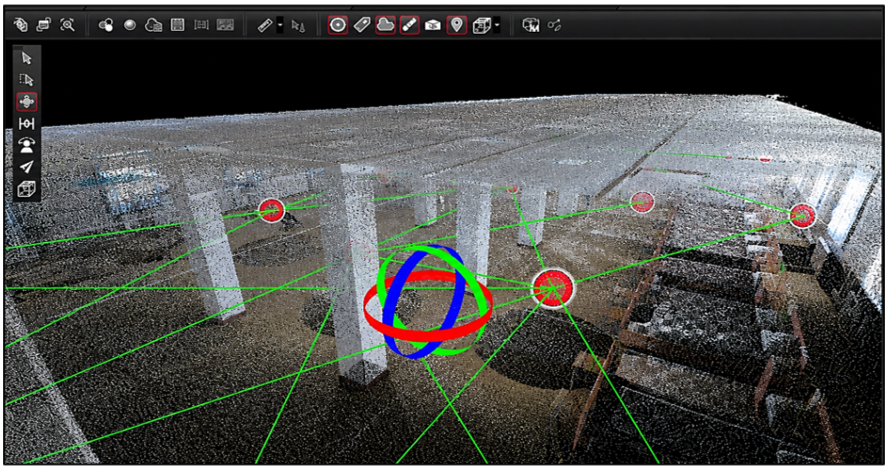

Figure 3. Registration connectivity graph in Cyclone REGISTER 360 PLUS

5 Discussion

The results show that the achieved accuracy depended not only on the scanner characteristics but also on the organization of the acquisition process. For a corridor interior, three factors were critical: regular overlap between adjacent stations, network reinforcement in repetitive segments, and two-stage QA. This combination, rather than the use of a specific commercial software package, is the main methodological outcome of the study.

The novelty of the paper is not the development of a new registration algorithm or hardware system. The novelty lies in a reproducible field and post-processing methodology for long corridor interiors. It also lies in the explicit integration of internal alignment metrics with independent metric verification and in the operational rules designed to reduce drift in repetitive geometry.

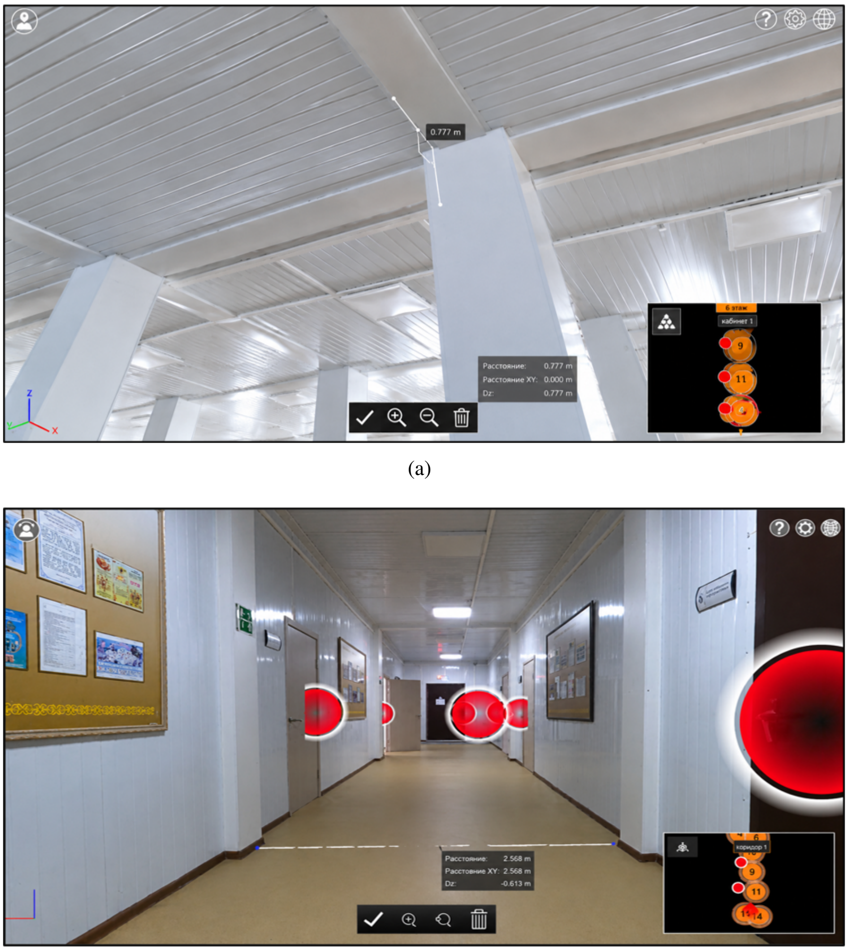

(a)

(b)

Figure 4. Examples of control measurements in TruView/Cyclone 3DR: (a) verification of horizontal distances; (b) measurement of linear parameters

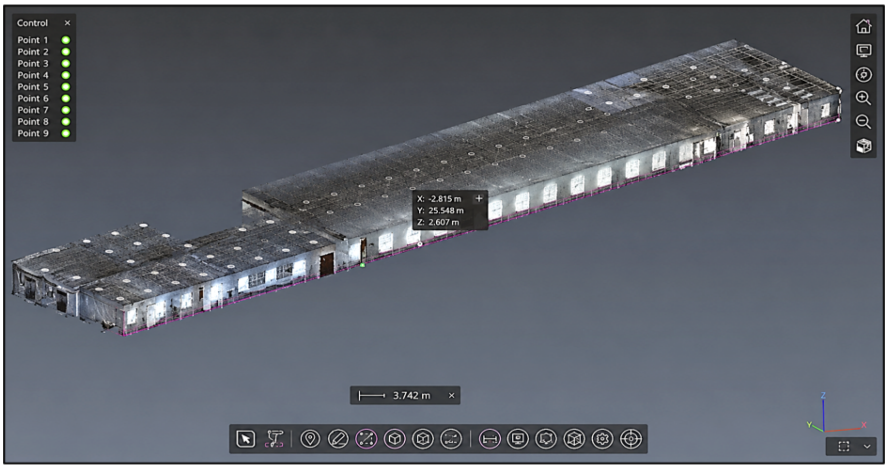

Figure 5. Final 3D model of the corridor interior and an example of a control measurement in Cyclone 3DR

The RMSE value of up to 5 mm should be interpreted in relation to the working scanning distance. The average working distance was approximately 5.8 m, and the maximum distance did not exceed 12.1 m. Therefore, the achieved accuracy is consistent with the specified characteristics of the BLK360 and reflects operation mainly at short and medium ranges.

Reflective surfaces, metal pipes, glossy floor coverings, and occasional dynamic objects were expected sources of local noise. Point cloud cleaning was therefore treated as a mandatory step affecting the final suitability of the data for engineering use. The cleaning procedure was described in detail to make this stage more transparent and reproducible.

The wording related to BIM and digital twins was refined. No parametric BIM model was created in this study. Therefore, the resulting point cloud should be described as input data for scan-to-BIM procedures and for subsequent digital representation of the interior, not as a completed digital twin.

The transferability of the proposed workflow to other layout schemes requires adaptation. In open spaces with fewer geometric landmarks, overlap should be increased and greater attention should be paid to natural or artificial control objects. In buildings with many small rooms, the network should be reinforced at door openings and local registration loops should be formed. Thus, the proposed approach is reproducible, but its parameters must be adjusted to the morphology of the object.

The limitations of the study include the use of a single object and the dependence of the post-processing pipeline on the commercial Leica software ecosystem. Nevertheless, the results include a histogram of control deviations, RMSE, P95, and maximum residual values. These metrics provide a more complete description of registration stability and independent metric verification. The main user decisions are largely software-independent and can be transferred to other TLS processing pipelines with appropriate adaptation.

6 Conclusion

This study proposed and validated a reproducible TLS-based workflow for three-dimensional modeling of a corridor-type building interior. The workflow combined controlled station overlap, local network reinforcement, adaptive setup height, registration graph inspection, removal of weak links, combined point cloud cleaning, and independent metric verification.

The obtained point cloud contained more than 100 million colorized points and demonstrated metric consistency suitable for engineering interpretation. Internal registration metrics were supported by independent control measurements, which confirmed agreement between the point cloud and in situ tape measurements within the 4–5 mm range.

The practical value of the study is the transparency and reproducibility of the acquisition and verification protocol. The results should be interpreted within the limits of the study because the workflow was tested on one corridor-type object and within the Leica software ecosystem. The resulting point cloud should therefore be regarded as metrically reliable input data for subsequent scan-to-BIM and related digital workflows, rather than as a finished BIM model or digital twin.

Author Contributions

Conceptualization, K.A. and A.S.; methodology, A.S. and A.M.; validation, A.S. and A.D.; formal analysis, A.S.; investigation, A.S. and A.M.; resources, K.A.; data curation, A.S. and A.D.; writing—original draft preparation, A.S.; writing—review and editing, A.M. and A.D.; visualization, A.S.; supervision, K.A.; project administration, K.A. All authors have read and agreed to the published version of the manuscript.

Fundings

This research was funded by the Science Committee of the Ministry of Science and Higher Education of the Republic of Kazakhstan (Grant no.: BR249011/0224).

Data Availability

The data used to support the findings of this study are available from the corresponding author upon request.

Conflicts of Interest

The authors declare no conflicts of interest.

References

[1] H. Macher, T. Landes, and P. Grussenmeyer, "From point clouds to building information models: 3D semi-automatic reconstruction of indoors of existing buildings," *Appl. Sci.*, vol. 7, no. 10, p. 1030, 2017. https://doi.org/10.3390/app7101030

[2] G. Rocha and L. Mateus, "A survey of scan-to-BIM practices in the AEC industry—A quantitative analysis," *ISPRS Int. J. Geo-Inf.*, vol. 10, no. 8, p. 564, 2021. https://doi.org/10.3390/ijgi10080564

[3] C. Gourguechon, H. Macher, and T. Landes, "Automation of as-built BIM creation from point cloud: An overview of research works focused on indoor environment," *ISPRS Arch. Photogramm. Remote Sens. Spat. Inf. Sci.*, vol. XLIII-B2-2022, pp. 193–200, 2022. https://doi.org/10.5194/isprs-archives-XLIII-B2-2022-193-2022

[4] Y. Zhang, L. Lu, X. Luo, and J. Pan, "Global BIM-point cloud registration and association for construction progress monitoring," *Autom. Constr.*, vol. 168, p. 105796, 2024. https://doi.org/10.1016/j.autcon.2024.105796

[5] H. Liu, D. Liu, and J. Chen, "Depth-informed point cloud-to-BIM registration for construction inspection using augmented reality," *Adv. Eng. Inform.*, vol. 62, p. 102867, 2024. https://doi.org/10.1016/j.aei.2024.102867

[6] J. Chen, S. Li, and W. Lu, "Align to locate: Registering photogrammetric point clouds to BIM for robust indoor localization," *Build. Environ.*, vol. 209, p. 108675, 2022. https://doi.org/10.1016/j.buildenv.2021.108675

[7] S. Park, S. Ju, M. H. Nguyen, S. Yoon, and J. Heo, "Automated point cloud registration approach optimized for a stop-and-go scanning system," *Sensors*, vol. 24, no. 1, p. 138, 2024. https://doi.org/10.3390/s24010138

[8] R. M. Túñez-Alcalde, M. S. A. Albadri, P. González-Cabaleiro, A. Fernández, and L. Díaz-Vilariño, "A top-down hierarchical approach for automatic indoor segmentation and connectivity detection," *ISPRS Ann. Photogramm. Remote Sens. Spat. Inf. Sci.*, vol. X-4/W5-2024, pp. 289–296, 2024. https://doi.org/10.5194/isprs-annals-X-4-W5-2024-289-2024

[9] D. Hu, V. J. L. Gan, and R. Zhai, "Automated BIM-to-scan point cloud semantic segmentation using a domain adaptation network with hybrid attention and whitening (DawNet)," *Autom. Constr.*, vol. 164, p. 105473, 2024. https://doi.org/10.1016/j.autcon.2024.105473

[10] D. Hu, V. J. L. Gan, and C. Yin, "Robot-assisted mobile scanning for automated 3D reconstruction and point cloud semantic segmentation of building interiors," *Autom. Constr.*, vol. 152, p. 104949, 2023. https://doi.org/10.1016/j.autcon.2023.104949

[11] B. Wang, C. Yin, H. Luo, J. C. P. Cheng, and Q. Wang, "Fully automated generation of parametric BIM for MEP scenes based on terrestrial laser scanning data," *Autom. Constr.*, vol. 125, p. 103615, 2021. https://doi.org/10.1016/j.autcon.2021.103615

[12] Q. Wang, P. Qian, Y. Liu, T. Li, L. Yang, and F. Yang, "Geometric accuracy evaluation method for subway stations based on 3D laser scanning," *Appl. Sci.*, vol. 12, no. 19, p. 9535, 2022. https://doi.org/10.3390/app12199535

[13] M. Jarząbek-Rychard and H. G. Maas, "Modeling of 3D geometry uncertainty in scan-to-BIM automatic indoor reconstruction," *Autom. Constr.*, vol. 154, p. 105002, 2023. https://doi.org/10.1016/j.autcon.2023.105002

[14] S. Isfort, M. Elias, and H. G. Maas, "Development and evaluation of a two-staged 3D keypoint based workflow for the co-registration of unstructured multi-temporal and multi-modal 3D point clouds," *ISPRS Ann. Photogramm. Remote Sens. Spat. Inf. Sci.*, vol. X-2-2024, pp. 113–120, 2024. https://doi.org/10.5194/isprs-annals-X-2-2024-113-2024

[15] A. Stefańska, H. Markowski, and S. Dixit, "Three-dimensional laser scanning for structure documentation and construction management: A case study of renovation and rebuilt of metro tunnels," *Ain Shams Eng. J.*, vol. 15, no. 5, p. 102665, 2024. https://doi.org/10.1016/j.asej.2024.102665

[16] ASTM International, "Standard specification for 3D imaging data exchange, version 1.0 (ASTM E2807-11(2019)e1)," 2019. https://store.astm.org/e2807-11r19e01.html

[17] International Organization for Standardization, "Organization and digitization of information about buildings and civil engineering works, including building information modelling (BIM)—Information management using building information modelling—Part 1: Concepts and principles (ISO 19650-1:2018)," 2018. https://www.iso.org/standard/68078.html

[18] Leica Geosystems, "Leica BLK360 imaging laser scanner," 2026. https://leica-geosystems.com/products/laser-scanners/scanners/leica-blk360